An Essential Phosphorylation-site Domain of Human cdc25C Interacts with Both 14-3-3 and Cyclins

May Morris, Annie Heitz, Jean Mery, Frederic Heitz, Gilles Divita

THE JOURNAL OF BIOLOGICAL CHEMISTRY
Vol. 275, No. 37, Issue of September 15, pp. 28849–28857, 2000
Printed in U.S.A.

An Essential Phosphorylation-site Domain of Human cdc25C Interacts with Both 14-3-3 and Cyclins*

Received for publication, April 7, 2000, and in revised form, June 16, 2000
Published, JBC Papers in Press, June 22, 2000, DOI 10.1074/jbc.M002942200

May C. Morris‡, Annie Heitz§, Jean Mery¶, Frederic Heitz¶, and Gilles Divita‡¶‖

From the ‡The Scripps Research Institute, Department of Molecular Biology, La Jolla, California 92037, §Center de Biochimie Structurale-CNRS (UMR 9955) and INSERM U 414, Faculté de Pharmacie, 15 Avenue Charles Flahault, 34060 Montpellier Cedex, France, and ¶Centre de Recherches de Biochimie Macromoléculaire, Biophysics unit, CNRS-UPR 1086, 1919 route de Mende, 34293 Montpellier Cedex 5, France

Human cdc25C is a dual-specificity phosphatase involved in the regulation of cell cycle progression in both unperturbed cells and in cells subject to DNA damage or replication checkpoints. In this study, we describe the structure-function relationship of an essential domain of human cdc25C that interacts with 14-3-3 proteins. We show that this domain is a bi-functional interactive motif that interacts with cyclins primarily through their P-box motif in addition to 14-3-3 proteins. Characterization of the structural features of this domain by NMR and circular dichroism reveals two distinct α helical moieties interconnected by a loop carrying the 14-3-3 binding site. Moreover, the helical folding is induced upon binding to 14-3-3, suggestive of a conformational regulation of this domain of cdc25C through interactions with partner proteins *in vivo*. Combining our structural and biochemical data, we propose a detailed model of the molecular mechanism of cdc25C regulation by differential association with 14-3-3 and cdc2-cyclin B.

Cdc25 protein phosphatases play important roles in the control of cell cycle progression in eukaryotes by activation of cyclin-dependent kinases (cdks)[1] through dephosphorylation of two conserved residues, Thr^{14} and Tyr^{15} (1, 2). In addition to their essential function in the normal cell cycle, cdc25 phosphatases are involved in the checkpoint-induced control of cell cycle progression (3–5). Finally, cdc25 phosphatases have been shown to possess an important oncogenic potential and to be overexpressed in a variety of cancers and cancer cell lines (6, 7). In humans three cdc25 isoforms exhibiting different structural and functional characteristics have been identified. Whereas cdc25A is involved in activation of cyclin-dependent kinases at the G_1/S transition (8–10), cdc25B and cdc25C both play important roles in activation of the G_2/M transition (6, 8, 11–15). The mitotic isoform cdc25C is regulated throughout the cell cycle by differential phosphorylation (15–19). Activation of human cdc25C at the G_2/M transition occurs concomitantly with phosphorylation of five serine/threonine-proline sites: Thr^{48}, Thr^{67}, Ser^{122}, Thr^{130}, and Ser^{214}, presumably by cdc2-cyclin B (15–17). In contrast, during interphase cdc25C is predominantly phosphorylated on Ser^{216} by protein kinase C-TAK1 (18, 19). Similarly, checkpoint-activated protein kinases cds1 and chk1 have been reported to phosphorylate cdc25C on Ser^{216} (3–5, 20–23). Phosphorylation of human cdc25C on Ser^{216} creates a consensus 14-3-3 binding site RS*X*pS*X*P (*X* being any amino acid; pS corresponding to phospho-Ser^{216}) (24–25), which represents an important regulatory motif affecting the fate of cdc25C both during a normal cell cycle and in the DNA damage and replication checkpoints (3–5, 18, 19). Recent studies in fission yeast, *Xenopus*, and mammalian cells reveal that this phosphorylation promotes binding of 14-3-3 proteins to cdc25 phosphatases *in vivo*, thus preventing their nuclear accumulation as well as their mitotic function (3–5, 26–30). In fission yeast, the 14-3-3 homolog Rad24 regulates the untimely nuclear localization of cdc25 by enhancing the nuclear export of cdc25 thanks to its nuclear export signal (26). In *Xenopus* and in human cells, in contrast, 14-3-3 proteins seem to promote the increased cytoplasmic retention of cdc25 by preventing recognition of the bipartite nuclear localization sequence (NLS) of cdc25 by the nuclear import machinery (27–30).

Despite these numerous studies, the molecular basis underlying the mechanism of regulation of cdc25 by 14-3-3 has still not been resolved. With the aim of investigating this issue, we used fluorescence spectroscopy, gel filtration, and affinity chromatography to examine the interactive properties of a 51-amino acid peptide, MP51, derived from residues 195 to 244 of human cdc25C that encompass the 14-3-3 binding site and the putative bipartite NLS (31). We found that this domain of cdc25C not only interacts with 14-3-3ζ *in vitro* and *in vivo* but also with human cyclins A and B1 with similar high affinity. We show that the interaction of MP51 with cyclins is primarily mediated through their P-box motif and is independent of MP51 phosphorylation, in contrast to the interaction between MP51 and 14-3-3ζ. Moreover we found that phosphorylation of both MP51 and full-length human cdc25C by cds1 favors the formation of stable MP51 and cdc25C·14-3-3 complexes over those of MP51- or cdc25C-cyclin B1 complexes both *in vitro* and *in vivo*. Finally, we examined the structural properties of MP51 by circular dichroism and NMR spectroscopy and propose the first structural model of an essential N-terminal regulatory domain of human cdc25C. The consequences of the dual functionality of this domain of human cdc25C are discussed with respect to its structural characteristics as a function of its phosphorylation status and in the context of cell cycle regulation.

* This work was supported by grants from the CNRS, l'Association de Recherche Contre le Cancer, and La Ligue de Recherche contre Le Cancer (to G. D.). The costs of publication of this article were defrayed in part by the payment of page charges. This article must therefore be hereby marked "*advertisement*" in accordance with 18 U.S.C. Section 1734 solely to indicate this fact.

‖To whom correspondence should be addressed: The Scripps Research Institute, Dept. of Molecular Biology, MB4, 10550 North Torrey Pines Rd., La Jolla, CA 92037. Tel.: 858-784-8065; Fax: 858-784-2277; E-mail: gilles@scripps.edu.

[1] The abbreviations used are: cdk, cyclin-dependent kinase; NLS, nuclear localization sequence; TFE, 2,2,2-trifluoroethanol; TOSCY, total correlation spectroscopy; NOE, nuclear Overhauser effect; NOESY, NOE spectroscopy; HSQC, heteronuclear correlation; GST, glutathione *S*-transferase.

EXPERIMENTAL PROCEDURES

Synthesis, Phosphorylation, and Purification of MP51—MP51 was synthesized by solid phase peptide synthesis according to the Fmoc (*N*-(9-fluorenyl)methoxycarbonyl)/*tert*-butyl strategy, then purified by ion exchange chromatography and semi-preparative high performance liquid chromatography as described previously (31). MP51 was identified by electrospray mass spectrometry and amino acid analysis. Stoichiometric phosphorylation of MP51 on Ser^{22} was performed using 1–5 μg of recombinant human GST-cds1 (kindly provided by Dr. C. McGowan) for 30 min at 37 °C in kinase buffer (50 mM Tris-HCl, pH 7.5, 100 mM NaCl, 10 mM $MgCl_2$, 2 mM ATP). After phosphorylation, MP51 was purified by gel filtration chromatography on a Superose 12 column and identified by mass spectrometry.

Circular Dichroism—CD spectra were recorded on a Jasco 800 dichrograph using 1-mm-thick quartz cells. MP51 or MP51P was initially diluted to a final concentration of 0.1 mg ml^{-1} in water or phosphate buffer (pH 7.0), and structural variations were measured as a function of changes in the initial CD spectrum upon addition of increasing concentrations of methanol or 2,2,2-trifluoroethanol (TFE). CD spectra were measured between 185 and 260 nm, and ellipticity values were calculated at 220 nm as described previously (32). For binding experiments, 14-3-3ζ was diluted to a final concentration of 8 μM in phosphate buffer, pH 7.0, and incubated for 15 min with a 2-fold excess of MP51 or MP51P. Data collection and analysis were performed with the package software from Jasco.

NMR Spectroscopy—NMR experiments were performed with samples containing 2 mM MP51 or MP51P in either H_2O/TFE-d_3 (2:1) or $H_2O/^2H_2O$/TFE-d_2 (57:10:33). Spectra were acquired on a Bruker AMX 600 spectrometer, equipped with q z-gradient triple resonance (^1H, ^{15}N, ^{13}C) probe at 290 and 305 K, and ^1H chemical shifts were referred to internal TSP-d4. Clean TOCSY (33) with 30- and 70-ms mixing times and NOESY (34) with 200- and 300-ms mixing times were used for proton assignments. Two-dimensional heteronuclear inverse-detected ^{13}C-^1H heteronuclear correlation (HSQC) (35) and HSQC-TOCSY spectra were recorded at natural abundance for carbon identification. The carrier frequency was centered on the water signal, and the solvent was suppressed by continuous low power irradiation during the relaxation delay and during the mixing time for NOESY spectra. Two-dimensional spectra were obtained using 2048 and 4096 points for each t1 value, and 512 t1 experiments were acquired. The spectral width was 10 ppm for proton and 165 ppm for ^{13}C. Before Fourier transform, the time domain data were multiplied by a phase-shifted sine bell or square-sine-bell window function in both dimensions. ^1H chemical shift assignments were achieved by standard two-dimensional sequence-specific methods (36). Assignments of α-carbons were determined by direct HSQC, and ambiguities were solved through remote connectivities obtained by homonuclear transfers in HSQC-TOCSY. The random coil chemical shift values used to calculate the chemical-shift index were those obtained in aqueous solution containing 30% v/v TFE (37). The methylene carbon of TFE was taken as reference at 61.70 ppm in ^{13}C spectra.

Secondary Structure Prediction and Modeling of MP51 —Secondary structure predictions of MP51, human cdc25B, and human cdc25A were carried out using the different methods available on the Institut de Biologie et Chimie des Proteines web server (Network Protein Sequence Analysis (NPSA)), including DSC, Gibrat, Levin, DPM, PREDATOR, and SOPMA (38). Based on both NMR data and secondary structure predictions, a three-dimensional model of the structure of MP51 was elaborated using BIOPOLYMER and DISCOVER available through INSIGHT II (MSI Inc. San Diego, CA).

Expression and Purification of Proteins—Human cdk1 and cdk2 and human cyclins A and B1 were overexpressed in *Escherichia coli* and purified as described previously (39, 40). pmal-human 14-3-3ζ (kindly provided by Dr. D. Fisher) was prepared as a maltose-binding fusion protein, and maltose-binding protein was removed with factor Xa. Human 14-3-3ζ was further purified by ion exchange chromatography on a Mono Q column. The P-box domain of human cyclin B1 (residues 183 to 237) was overexpressed in *E. coli* and purified as a maltose-binding fusion protein. Full-length human cdc25C was prepared as described previously (40). GST-Nter-cdc25C (residues 1 to 302) was overexpressed in *E. coli* and purified as a GST fusion protein. For fluorescence experiments, the GST tag was cleaved with thrombin, and Nter-cdc25C was further purified by ion exchange chromatography on a Resource Q column (Amersham Pharmacia Biotech). Both full-length cdc25C and Nter-cdc25C were phosphorylated with recombinant human GST-cds1 for 30 min at 37 °C in a kinase buffer (50 mM Tris-HCl, pH 7.5, 100 NaCl, 10 mM $MgCl_2$, 2 mM ATP). After phosphorylation, cdc25C and Nter-cdc25C were purified by affinity chromatography on a GST trap column and by gel filtration chromatography on a Superose 12 column. Protein concentrations were routinely determined using the BCA protein assay reagent kit (Pierce) using bovine serum albumin as a standard.

Complexes formed between MP51 or MP51P and cyclin B1 or 14-3-3ζ were purified by size exclusion chromatography using either a Bio-Sil TSK 125 column (Bio-Rad) or a Superose 12 column (Amersham Pharmacia Biotech). Cyclin B1 and/or 14-3-3ζ were incubated with a 2-fold excess of peptide for 30 min at 25 °C in 50 mM potassium phosphate buffer, pH 7.5, containing 150 mM NaCl. Chromatographies were performed in the same buffer at a flow rate of 1 ml/min, and peak fractions were analyzed by SDS-polyacrylamide gel electrophoresis. A similar procedure was used to purify complexes formed between phosphorylated full-length cdc25C and cyclin B1 or 14-3-3ζ.

Fluorescence Binding Experiments—Fluorescence measurements were performed at 25 °C using a PTI spectrofluorometer, with spectral bandpasses of 4 nm for both excitation and emission in a fluorescence buffer containing 150 mM potassium phosphate, pH 7.2, 1 mM EDTA, 5% glycerol. Binding experiments were performed by tryptophan fluorescence spectroscopy essentially as described previously (39, 40). Intrinsic tryptophan fluorescence was excited at 290 nm, and emission spectra were recorded between 310 and 400 nm. Recombinant cdks, cyclins, cdk-cyclin complexes, and human 14-3-3ζ were incubated in fluorescence buffer for 30 min, and titration experiments were initiated by the addition of increasing concentrations of peptide (MP51, MP51P) or proteins (cdc25C, Nter-cdc25) to a fixed concentration of these proteins (100 nM). Measurements were corrected and fitted according to a standard quadratic equation using the Grafit software (Erathicus software Ltd) as described previously (39, 40).

Pull-down Experiments—1 mg of MP51 and MP51P were crosslinked to 1 ml of epoxy-activated Sepharose 6B resin. 1 mg of unphosphorylated and phosphorylated GST-Nter cdc25C was coupled to 1 ml of GST Sepharose 4B resin. For pull-down experiments with recombinant proteins, 10 μg of purified cdks, cyclins, or 14-3-3ζ were incubated for 15 min with the beads in 10 mM Tris-HCl, pH 7, 250 mM NaCl, 1 mM EDTA, then washed twice in the same buffer. For pull-down experiments with cell lysates, extracts were prepared in radioimmune precipitation buffer-SDS from asynchronous HS68 fibroblasts cultured to 70% confluency in Dulbecco's modified Eagle's medium (Life Technologies, Inc.) supplemented with 10% fetal calf serum (Life Technologies, Inc.) as described previously (16). Total extracts were incubated for 15 min with the beads in radioimmune precipitation buffer-SDS, then extensively washed in the same buffer. Proteins retained on the different beads were analyzed by Western blotting with polyclonal rabbit antibodies against 14-3-3ϵ (sc-1020), cyclin A (sc-751), cyclin B1 (sc-752), cdc2 (sc-747), and cdk2 (sc-748) (Santa Cruz Biotechnology Inc.).

RESULTS

Binding of MP51 to 14-3-3—With the aim of dissecting the mechanism of cdc25C regulation by 14-3-3 at the molecular level, we took advantage of the absence of tryptophan groups in MP51 and of the presence of highly conserved tryptophan residues in 14-3-3 proteins to monitor and quantify their interactions by intrinsic fluorescence spectroscopy. 14-3-3 proteins indeed contain two well conserved tryptophan residues, Trp^{59} (located in helix C) and Trp^{228} (in helix I), which form, respectively, the floor and the wall of the channel in the x-ray structure of 14-3-3 (25, 41, 42). As previously documented (31) and as shown in Fig. 1*a*, the addition of increasing concentrations of unphosphorylated MP51 to 14-3-3ζ induced quenching of its intrinsic fluorescence by 40%, and curve-fitting yielded a K_d value of 132 nM ± 25. Moreover, we were able to purify stable complexes of unphosphorylated MP51·14-3-3ζ by gel filtration chromatography in the presence of a high concentration of salt, revealing that the interactions are mainly hydrophobic (Fig. 2*a*). The same experiment performed with MP51 phosphorylated on Ser^{22}, denoted MP51P, induced a similar quenching of fluorescence, but a 6-fold higher affinity for 14-3-3ζ, with a K_d value of 21 ± 9 nM, revealing the pivotal role of phosphorylation of Ser^{22} in this interaction. However, the observation that MP51 peptide can interact with 14-3-3ζ *in vitro* in the absence of phosphorylation suggests that initial interactions occur through residues other than phospho-Ser^{22}. The significant

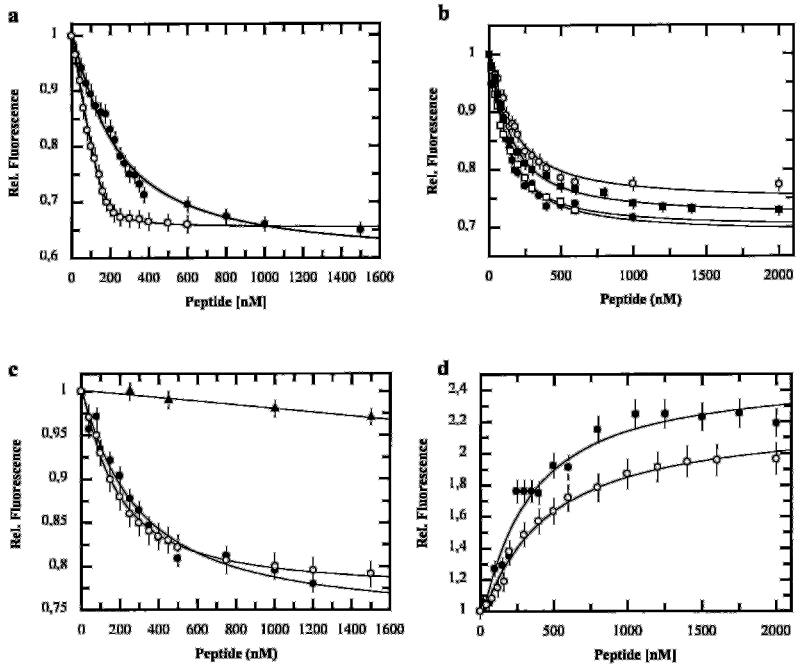

FIG. 1. **Binding of MP51 and MP51P to 14-3-3ζ, cdks, and cyclins.** *a*, binding of MP51 and MP51P to human 14-3-3ζ. 100 nM human 14-3-3ζ protein was incubated at 25 °C in potassium phosphate buffer (150 mM potassium phosphate, pH 7.2, 1 mM EDTA, 5% glycerol), and changes in its intrinsic tryptophan fluorescence were measured upon the addition of increasing concentrations of MP51 (●) or MP51P (○). *b*, binding of MP51 and MP51P to human cyclins. 100 nM human cyclin B1 was titrated with increasing concentrations of MP51 (●) or MP51P (○); 100 nM human cyclin A was titrated with increasing concentrations of MP51 (■) or MP51P (□). Binding of peptides was monitored by following the quenching of intrinsic fluorescence of cyclins at 330 nm. *c*, binding of MP51 (●) and MP51P (○) to the P-box of human cyclin B1. Experiments were performed as described for cyclin B1 using 100 nM P-box purified as a maltose-binding fusion protein or maltose-binding protein as a control (▲). *d*, binding of MP51 and MP51P to human cdk2. 100 nM human cdk2 was titrated with increasing concentrations of MP51 (●) or MP51P (○), and binding was monitored as the increase in the intrinsic fluorescence of human cdk2 at 340 nm. In all the cases values measured for different concentrations of peptide are shown together with their best-fitting curve, corresponding to an average of four separate experiments.

quenching of fluorescence observed in these experiments indicates that direct contacts between residues of MP51 and the Trp groups of 14-3-3ζ are involved. Moreover, curve-fitting reveals that two molecules of MP51 or MP51P bind per 14-3-3ζ dimer, indicating that the two binding sites in the 14-3-3ζ dimer are accessible and that binding of MP51 peptide to one site does not exclude binding to the other, as already documented for short 14-3-3 binding peptides containing tandem phospho-serine motifs (25). In comparison, as reported in Table I, unphosphorylated recombinant full-length cdc25C and the N-terminal domain of cdc25C, denoted Nter-cdc25C, interacted very poorly with 14-3-3ζ, whereas their phosphorylation by cds1 designated pcdc25C and pNter-cdc25C promoted their high affinity interaction with 14-3-3ζ, with K_d values of 57 ± 5 nM and 48 ± 7 nM, respectively, and a stoichiometry of 1 per 14-3-3ζ dimer.

Binding of MP51 to cdks and Cyclins—We next investigated the potential of unphosphorylated and phosphorylated MP51 to interact with human cyclins A and B1 as well as with their cdk partners cdk1 and cdk2 *in vitro* by intrinsic fluorescence spectroscopy and gel filtration chromatography. Like 14-3-3 proteins, both cdks and cyclins are characterized by the presence of several conserved Trp groups (39). As shown in Fig. 1*b*, upon addition of either MP51 or MP51P the intrinsic fluorescence of cyclins A and B1 was quenched by about 25 to 30%. Fitting of the titration curves revealed that MP51 presents a high affinity for both cyclin A and B1 with dissociation constant values of 151 ± 23 nM and 110 ± 14 nM, respectively. Similar affinities were obtained with MP51P (Table I), revealing that binding of MP51 to cyclins is not regulated by phosphorylation of Ser^{22}. The stability of MP51-cyclin B1 complexes was further confirmed by size exclusion chromatography, as reported in Fig. 2*b*. That these complexes remain stable in the presence of a high concentration of salt indicates that the interaction between MP51 and cyclin B1 involves mainly hydrophobic contacts. Interestingly, we have previously shown that full-length recombinant human cdc25C interacts with cyclins A and B1 with very similar K_d values, *i.e.* 72 ± 4.5 nM and 85 ± 9 nM, respectively (40). As such, these data suggest that MP51 is the main domain in cdc25C involved in high affinity interactions with cyclins. At least two studies have shown that a well defined motif in cyclin B1, the P-box, is an essential domain required for the cdc25-dependent dephosphorylation of cdc2-cyclin B at the G_2/M transition and may serve as an activator of cdc25 phosphatases "in trans" (8, 43). We have previously suggested that human cdc25C might interact physically with this motif (40). Like cyclins, the P-box is characterized by the presence of a conserved tryptophan group, of which we took advantage to investigate whether MP51 could interact with the P-box by fluorescence spectroscopy. As shown in Fig. 1*c*, the addition of increasing concentrations of MP51 to a maltose-binding protein-P-box fusion protein induced quenching of its intrinsic tryptophan fluorescence by 20%, whereas maltose-binding protein alone did not interact with MP51. These results indicate that the P-box motif and the MP51 motif of human cdc25C interact directly, and curve-fitting yielded a dissociation constant for this interaction of ~300 nM. As for full-length cyclin B1, binding of MP51 to the P-box was not regulated by phosphorylation on Ser^{22} (Table I). We also demonstrated that recombinant full-length and Nter-cdc25C formed stable complexes with cyclin B1 and with its P-box independently of phosphorylation (Table I).These results show for the first time that the P-box domain of cyclin B1 interacts physically with human cdc25C and that MP51 is likely to be the main domain of cdc25C involved in this interaction. However, comparison of the dissociation constants for the different interactions indi-

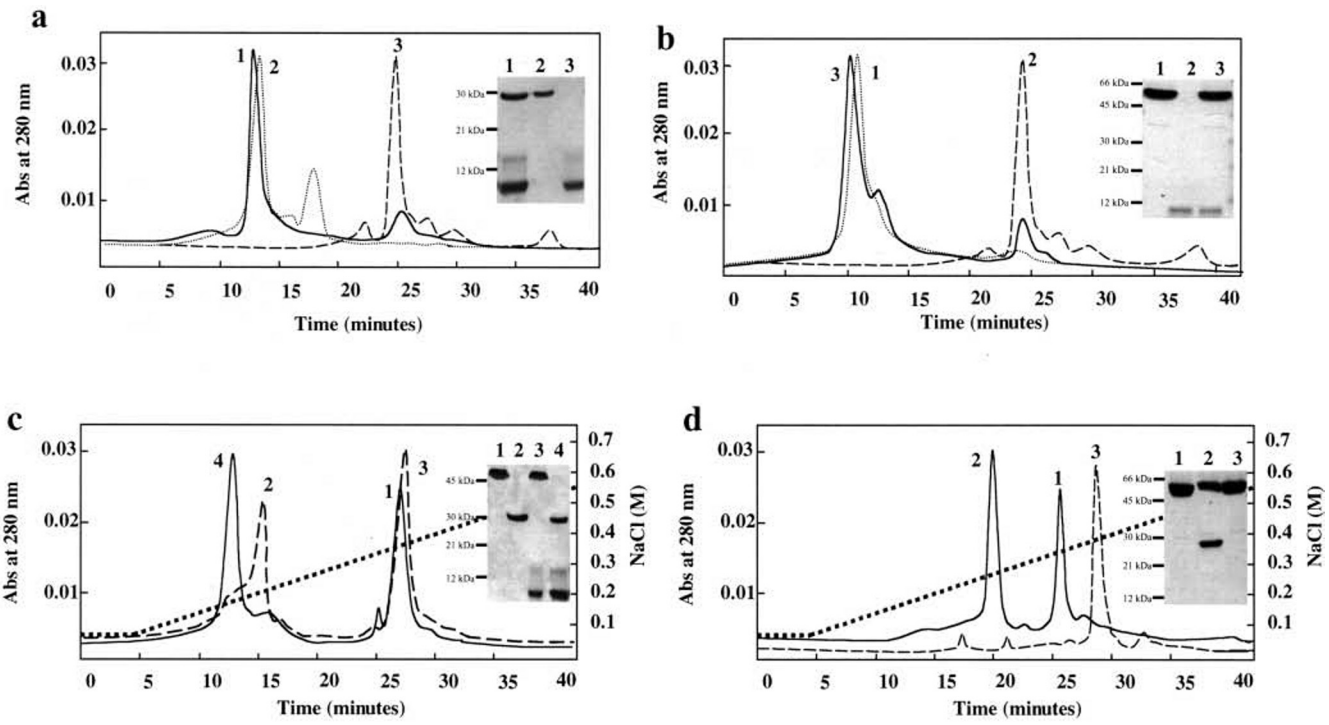

FIG. 2. **Purification of MP51·14-3-3ζ, MP51·cyclin B1, and full-length cdc25C·14-3-3ζ complexes.** *a*, purification of MP51·14-3-3ζ complexes by size exclusion chromatography. 14-3-3ζ eluted in a major peak at 13 min (*2*), and uncomplexed MP51 eluted in a peak at 25 min (*3*). MP51·14-3-3ζ complexes eluted in a single peak at 12 min (*1*). The identity of the entities eluting in each peak, shown in the insert, was determined by Coomassie Blue staining following electrophoresis on a 15% SDS-polyacrylamide gel. *b*, purification of MP51-cyclin B1 complexes by size exclusion chromatography. Cyclin B1 eluted in a single peak after 11 min (*1*), uncomplexed MP51 eluted in a peak at 25 min (*2*), and MP51-cyclin B1 complexes eluted in a single peak after 10 min (*3*). The identity of the entities eluting in each peak was determined as in *panel a*, as shown in the insert. *c*, displacement experiments. MP51-cyclin B1 and MP51P-cyclin B1 complexes were first purified by size exclusion chromatography as described in *panel b*, then incubated for 15 min at 25 °C in the presence of a stoichiometric concentration of 14-3-3ζ. Complexes were then separated by cation exchange chromatography on a Mono Q column in phosphate buffer pH 7.5 and eluted in a linear gradient of NaCl. Incubation of MP51-cyclin B1 with 14-3-3ζ (*dashed line*) resulted in the elution of two main peaks at 200 mM (*2*) and 370 mM (*3*) NaCl, corresponding, respectively, to 14-3-3ζ and to the MP51-cyclin B1 complex. Incubation of MP51P-cyclin B1 with 14-3-3ζ (*solid line*) led to the elution of two major peaks at 170 mM (*4*) and 350 mM (*1*) NaCl containing, respectively, MP51P·14-3-3ζ and monomeric cyclin B1. The identity of the entities eluting in each peak was determined as in *panel a*, as shown in the insert. *d*, Hu-pcdc25·14-3-3ζ and Hu-pcdc25C-cyclin B1 complexes were separated by cation exchange chromatography as described in *panel* c. Incubation of Hu-pcdc25·14-3-3ζ with cyclin B1 and incubation of Hu-pcdc25C-cyclin B1 with 14-3-3ζ, both, resulted in the elution of two major peaks (*solid line*) at 270 mM (*2*) and 350 mM (*1*) NaCl, corresponding, respectively, to Hu-pcdc25·14-3-3ζ and to cyclin B1. Monomeric Hu-pcdc25C was eluted with 380–400 mM (*3*) NaCl (*dashed line*). *Abs*, absorbance.

TABLE I

Affinity constants of peptides and cdc25C for 14–3-3, cyclin B1, and the P-box domain

K_d values (in nM) were determined by monitoring the quenching of intrinsic fluorescence. The data reported here correspond to averages of four independent experiments.

	MP51		Nter-cdc25C		cdc25C	
	Ser^{22}	$pSer^{22}$	Ser^{216}	$pSer^{216}$	Ser^{216}	$pSer^{216}$
14–3-3ζ	132 ± 25	21 ± 9	400 ± 78	48 ± 7	1200 ± 234	57 ± 5
Cyclin B1	110 ± 14	85 ± 4	78 ± 7	82 ± 10	85 ± 6	80 ± 4
P-Box	300 ± 45	282 ± 39	178 ± 13	185 ± 28	162 ± 17	186 ± 15

cates that other residues within the N-terminal, regulatory domain of cdc25C as well as other domains of cyclin B1 must be involved in secondary interactions between these two proteins.

We have previously shown that *in vitro*, recombinant full-length cdc25C interacts with monomeric cyclins with high affinity but with monomeric cdks with low substrate-enzyme affinity and with preformed cdk-cyclin complexes with intermediate, cooperative affinity, suggesting that *in vivo* the interaction between cdc25C and cdk-cyclin complexes is primarily mediated by the interaction between cdc25C and the cyclin (40). We therefore examined to what extent MP51 could interact with cdks and cdk-cyclin complexes. As shown in Fig. 1*d*, the addition of MP51 to cdk2 or cdk1 (data not shown for the latter) induced an increase in their intrinsic fluorescence by a factor of 1.5 to 2.2. Best fits for titration curves yielded K_d values of 568 ± 100 nM for cdk1 and 510 ± 95 nM for cdk2 in the same range as those reported for full-length cdc25C (40), indicative of a similar substrate-enzyme interaction. In contrast, the affinity of MP51 for preformed cdk-cyclin complexes is relatively low compared with that of full-length cdc25C (40), with K_d values of 1.2 μM for cdk2-cyclin A and 0.8 μM for cdk1-cyclin B1 (data not shown). These results indicate that although MP51 peptide is able to interact with monomeric cyclins and monomeric cdks *in vitro*, it is unable to interact cooperatively with both components in the cdk-cyclin complex in the absence of other domains of full-length cdc25C. The micromolar affinity measured between MP51 and cdk-cyclin complexes suggests a typical transient substrate-enzyme interaction, as previously determined for histone H1 (44). In support of this hypothesis, we were indeed able to phosphorylate MP51 on Ser^{20} using active cyclin-dependent kinase immunoprecipitated from cell extracts (data not shown).

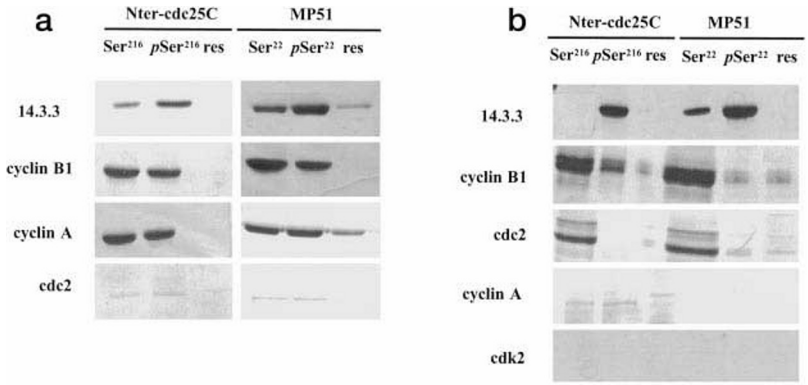

FIG. 3. ***In vitro* and *in vivo* pull-down experiments.** Pull-down experiments were performed with unphosphorylated or phosphorylated GST-Nter-cdc25C and MP51 coupled to GST-Sepharose 4B and epoxy-activated Sepharose 6B resin, respectively. *a*, pull-down experiments carried out with recombinant proteins. *b*, pull-down experiments performed with total cell extracts from asynchronous HS68 fibroblasts. *Ser*^{216}, unphosphorylated on Ser^{216}; *p Ser*^{216}, phosphorylated on Ser^{216} by cds1; *res*, uncoupled resin. 14-3-3ζ, cyclin A, cyclin B1, cdc2, and cdk2 retained by Nter-cdc25C and MP51 were detected by Western blotting.

Differential Binding of MP51 to 14-3-3ζ and to Cyclin B1—To understand the dual ability of MP51 to interact with 14-3-3ζ and cyclins, we devised the following experiment. Purified MP51 or MP51P-cyclin B1 and MP51 or MP51P·14-3-3ζ complexes were incubated with an equimolar concentration of either 14-3-3ζ or cyclin B1, respectively, then subjected to chromatographic separation. Because these complexes are very similar in size, we chose to discriminate them by ion-exchange chromatography rather than by gel filtration chromatography. In phosphate buffer pH 7.5 containing 75 mM NaCl, neither MP51 nor MP51P bound to the column, whereas 14-3-3ζ and cyclin B1 bound efficiently and were eluted with 130 mM and 340 mM NaCl, respectively. As shown in Fig. 2*c*, when MP51-cyclinB1 complexes were incubated with 14-3-3ζ, subsequent chromatographic separation yielded two main peaks, the one containing 14-3-3ζ and the other MP51-cyclinB1 complexes. When the same experiment was performed with purified MP51P-cyclin B1 complexes, 14-3-3ζ disrupted this interaction and displaced most of MP51P from the cyclin to form highly stable MP51P·14-3-3ζ complexes. These results clearly show that phosphorylation of Ser^{22} favors the interaction between MP51 and 14-3-3ζ over that with cyclin B1, as expected from the respective K_d values, and is essential for displacing MP51 from cyclins to 14-3-3 proteins. Moreover, they reveal that phospho-Ser^{22} is still accessible for 14-3-3ζ when MP51P is bound to cyclin B1. In contrast, when the converse experiments were performed with either MP51 or MP51P bound to 14-3-3ζ, cyclin B1 (even in five-fold excess) was unable to displace them, suggesting that most of the peptide is masked and inaccessible for cyclin B1 once bound to 14-3-3ζ (data not shown). To address the relevance of these results with respect to full-length cdc25C, we performed essentially the same experiments using full-length cdc25C phosphorylated by cds1. As shown in Fig. 2*d*, the addition of a 5-fold excess of cyclin B1 was not sufficient to promote the disruption of highly stable pcdc25C·14-3-3ζ complexes. In contrast, the addition of a 2-fold excess of 14-3-3ζ led to the displacement of cyclin B1 from preformed pcdc25C-cyclin B1 complexes to produce pcdc25C·14-3-3ζ complexes. These data indicate that full-length cdc25C behaves essentially like MP51 in its ability to associate differentially with both 14-3-3ζ and cyclin B1, binding to the former being favored and stabilized by phosphorylation on Ser^{216}.

Physiological Binding of MP51 and cdc25C to 14-3-3 and cdc2-Cyclin B—To address the physiological relevance of the interactions described above, we examined the ability of MP51 and of Nter-cdc25C to bind 14-3-3 and cdk-cyclin complexes from total extracts of human HS68 fibroblasts. MP51 and MP51P were cross-linked to epoxy-activated Sepharose resin, whereas unphosphorylated and phosphorylated GST-Nter-cdc25C were coupled to GST-Sepharose resin. We first verified the ability of these beads to retain either recombinant 14-3-3, cyclins, or cdks. As shown in Fig. 3*a*, 14-3-3ζ was preferentially retained by the phosphorylated forms of MP51 and Nter-cdc25C and bound the unphosphorylated beads with a lower affinity. In contrast, monomeric recombinant cyclins A and B were similarly retained by both phosphorylated and unphosphorylated beads. Finally, in the absence of cyclins, monomeric recombinant cdc2 was not retained by any of these beads, consistent with the idea that the interaction between cdc25C and cdks is of a weak enzyme-substrate type and requires the presence of cyclin for stabilization. In all cases, the interactions observed were consistent with the K_d values obtained by fluorescence spectroscopy.

We next examined whether a differential binding behavior could be observed between endogenous 14-3-3 and cdk-cyclin complexes upon incubation of the phosphorylated or unphosphorylated beads with total cell lysates of HS68 fibroblasts. As shown in Fig. 3*b*, 14-3-3ϵ bound exclusively to phosphorylated Nter-cdc25C and preferentially to MP51P, although a residual fraction also bound to MP51. In contrast, cyclin B and cdc2 were preferentially retained by the unphosphorylated beads. A variable, residual fraction of cyclin B could also be detected associated to the phosphorylated beads, suggesting that all 14-3-3ϵ had been titrated out of the extract and that an excess of cdc25C protein or peptide was available to bind some cyclin B. Interestingly, although cdc2-cyclin B complexes were specifically retained by MP51 and Nter-cdc25C, cdk2-cyclin A complexes were not, reflecting the *in vivo* specificity of the cdc25C isoform for mitotic cdc2-cyclin B complexes. These results clearly demonstrate that *in vivo*, phosphorylation of cdc25C on Ser^{216} favors the interaction between cdc25C and 14-3-3 over that with cdc2-cyclin B complexes.

Structural Characterization of MP51—Secondary structure prediction of MP51 was carried out using different methods available on the NPSA IBCP web server. Analysis of the different predictions and comparison with the consensus secondary structure prediction for MP51 reported in Fig. 4*a* reveal that two helical domains are systematically predicted with high accuracy by all methods. The first helix encompasses residues Glu^{2} to Val^{12} in MP51, the second, residues Arg^{31} to Lys^{39}. The two serines of MP51, Ser^{20} and Ser^{22}, corresponding to phosphorylation sites Ser^{214} and Ser^{216} in human cdc25C, are located in a loop that connects these two predicted helices.

The structure of MP51 and MP51P were determined by

a

```
                5    10   15   20   25   30   35   40   45   50
                |    |    |    |    |    |    |    |    |    |
MP51            MEFSLKDQEAKVSRSGLYRSPSMPENLNRPRLKQVEKFKDNTIPDKVKKKC
DPM             hhhhhhhhhhhh                hhhhhhhhhh       h
DSC               hh                        hhhhhhhh         eeee
GOR             hhhhhhhhhhhh                hhhhhhhhhhh  h hhhhhhhh
HNNC            hhhhhhhhhhhh                  hhhhhhh       hhhhhhh
Predator        hhhhhhhhhh                    hhhhhhh
SIMPA96         hhhhhhhhhh  hhhhh             hhhhhhhhh     hhhhhhh
SOPMA           hhhhhhhhhhhhhhh                 hhhhhhhhh       hh
Cons struct      hhhhhhhhhhhh                 hhhhhhhhhh        hh
NMR struct         hhhhhhhhhhhhh              hhhhhhhhhhhhh
```

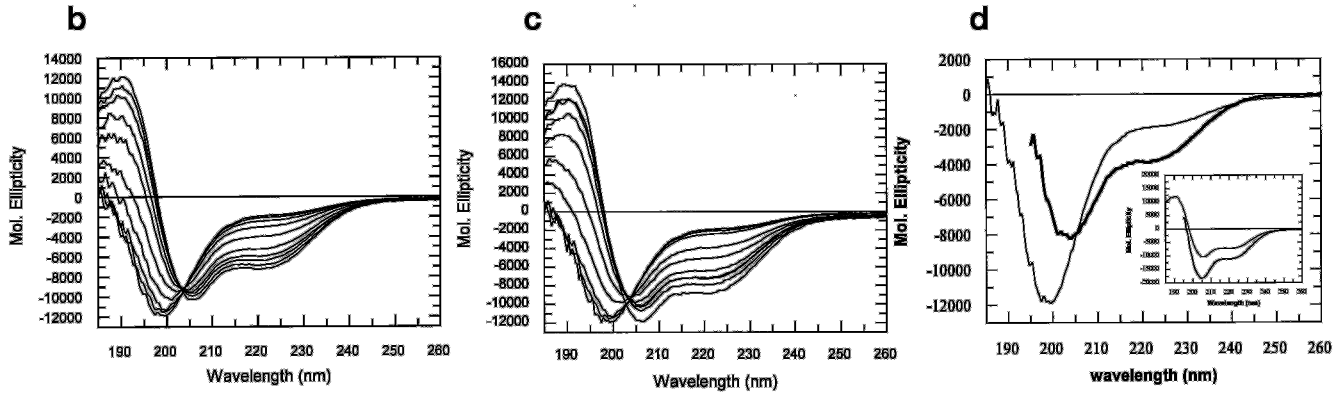

FIG. 4. **Secondary structure of MP51.** *a*, the secondary structure of MP51 was predicted using the methods available through the IBCP web server, including DPM, DSC, GOR, HNNC, Predator, SIMPA96, SOPMA. α-Helices and β-strands are defined by *h* and *e*, respectively. Comparison of the different predictions led to a consensus secondary structure prediction: *Cons struct* and *NMR struct* presents the location of the α-helices determined by NMR. Formation of secondary structures in MP51 (*b*) and MP51P (*c*) was analyzed by circular dichroism at 25 °C in TFE. MP51 and MP51P were diluted in water to a final concentration of 0.1 mg ml^{-1}, and increasing concentrations of TFE were incrementally added (0, 5, 9, 15, 20, 26, 30, 38, 44, and 50%). CD data were measured between 185 and 260 nm. *d*, secondary structure of MP51 complexed to 14-3-3ζ. 14-3-3ζ protein was diluted to a final concentration of 8 μM in phosphate buffer pH 7.0 and incubated with 16 μM of MP51. CD spectra for 14-3-3ζ and 14-3-3ζ·MP51 complexes (*bold line*) were recorded after 15 min (*inset*). The differential spectrum of MP51 bound to 14-3-3ζ was calculated and analyzed using the Jasco software package and is shown (*bold line*) together with that of monomeric MP51.

circular dichroism and NMR. We have previously shown that MP51 does not adopt any typical secondary folds in aqueous solution but, instead, multiconformational states (31). Moreover we did not observe any detectable changes in the α-helical content of MP51 following stoichiometric phosphorylation on Ser^{22} by recombinant cds1 (Fig. 4*c*). However, the addition of increasing concentrations of TFE stabilized α-helical structures in both MP51 and MP51P, as revealed by the characteristic CD spectra with two minima, 208 and 222 nm, associated with a maximum at 193 nm (Fig. 4, *b* and *c*). TFE induced conformational transitions that stabilized in a final plateau, with a first transition at a concentration of 30%, characterized by an α-helical content of about 50%, essentially as expected from the secondary structure predictions. That the peptide is ordered in α-helices when the hydrophobicity of its environment is increased is a good indication that it may fold when surrounded by the rest of cdc25C or when interacting with partner proteins as has been described for several proteins involved in important cellular functions (45). To address this possibility, we examined the structural status of MP51 and MP51P bound to 14-3-3ζ by CD. As shown in Fig. 4*d*, the spectrum of 14-3-3ζ is characteristic of a structured protein with a high α-helical content. The spectrum of MP51 obtained by substraction of the spectrum of 14-3-3ζ from that of a MP51·14-3-3ζ complex in a 2:1 ratio is characterized by two minima at 208 and 222 nm, indicating that MP51 adopts an α-helical conformation when bound to 14-3-3ζ. Calculation of the ellipticity of MP51 (or MP51P) bound to 14-3-3ζ yields an α-helical content of about 50%, consistent with our secondary structure predictions and corresponding to the folding ratio obtained in 30% TFE.

Further characterization of the structured domains of MP51 was undertaken by ^{1}H and ^{13}C NMR in water/TFE (2:1), which mimicked the folding induced through binding of 14-3-3ζ (Fig. 5). All residues were found to be in a trans conformation. The detection of strong dNN as well as dαN(i, i+3) and dαβ(i, i+3) NOEs from residues Leu^{5} to Tyr^{18} on the one hand and Arg^{31} to Ile^{43} on the other revealed the existence of two separate entities within MP51 that adopt an α-helical conformation. Examination of α-carbons by the chemical shift index method (46) showed a good correlation between the localization of the two helical entities in the chemical shift index profile and those deduced from the NOE pattern. In addition, both helical domains matched perfectly those determined by secondary structure prediction, and the percentage of residues determined as involved in α-helical structures corresponded perfectly to the 50% value determined by CD. Taken together, these data reveal that MP51 is composed of two separate α-helical motifs from residues 5 to 18 and 31 to 43 interconnected by a non-structured loop which carries phosphorylation sites Ser^{20} and Ser^{22}. Unfortunately no inter-helix NOEs could be detected, probably because of the presence of organic solvent, which precludes hydrophobic interactions within the peptide. Given that TFE has been shown to stabilize α-helices in peptides that have an intrinsic potential to form α-helices, but not to induce new, non-existent α-helical structures (47), and that MP51 adopts an α−helical structure when bound to 14-3-3ζ, we propose that similar helical domains are likely to exist in full-length human cdc25C. Essentially the same structural data were obtained for MP51P, including the trans conformation found for all residues in MP51.

Based on the data obtained by NMR and by secondary struc-

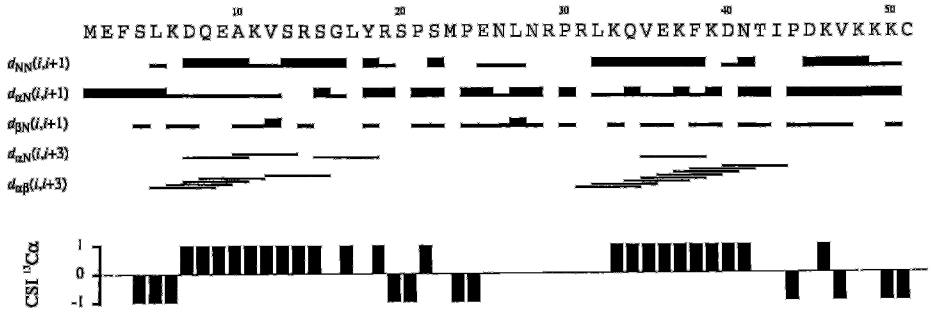

FIG. 5. **NMR structure of MP51.** Summary of the sequential and medium range NOE (*top*). Chemical shift index (*CIS*) of α-carbon resonances (*bottom*).

ture predictions, a three-dimensional model of the structure of MP51 was elaborated (Fig. 6*a*). This model highlights the two α-helices determined by NMR (α1 from Leu^5 to Tyr^{18}; α2 from Arg^{31} to Ile^{43}) as well as phospho-Ser^{22} and Pro^{24} located in the interconnecting loop. Residues 33 to 37 and 46 to 50 of MP51, corresponding to the bipartite NLS of human cdc25C, are located in part in the amphipathic α2-helix and in part in the unfolded C terminus of the peptide. Interestingly, projection of α2-helix shows that the lysine residues in the first moiety of the NLS (Lys^{33} and Lys^{37}) are located on the same side of the helix, whereas hydrophobic residues (Leu^{32}, Val^{35}, Ile^{43}) are located on the other. In addition, α2-helix is located between two proline residues, Pro^{30} and Pro^{44}, which appear to induce a breakage in the peptide structure, thereby positioning all the residues of the NLS on one same side of the structure, as shown in the surface representation in Fig. 6*b*. Interestingly, alignment of the primary sequence and secondary structure prediction of the three human cdc25 isoforms suggests that cdc25B and cdc25C, but not cdc25A, share this common structural organization in the 14-3-3 binding domain, with two α-helices interconnected by a loop carrying the canonical 14-3-3 binding site (Fig. 6, *c* and *d*).

DISCUSSION

Binding Properties of MP51—Interaction of cdc25 phosphatases with 14-3-3 proteins has been shown to play a critical role in cell cycle progression and checkpoint control, and it is now common knowledge that cdc25 proteins interact with 14-3-3 isoforms both *in vitro* and *in vivo* (26–31). In this study, we have shown that the MP51 domain of cdc25C interacts and forms stable complexes with 14-3-3ζ *in vitro* and *in vivo* in the absence of phosphorylation, suggesting that residues other than phospho-Ser^{22} are involved in this interaction, although phosphorylation of Ser^{22} dramatically increases its stability, consistent with previous *in vitro* studies with Raf-derived peptides (25, 48, 49). *In vivo*, however, mutation of this serine to alanine completely prevents co-immunoprecipitation of 14-3-3 proteins with cdc25 phosphatases from cell extracts (26–30), and *in vitro* we similarly observed a very weak interaction between 14-3-3ζ and unphosphorylated recombinant Nter- or full-length cdc25C, whereas the phosphorylated counterparts formed highly stable complexes. This discrepancy most likely reflects conformational constraints present in the full-length protein, which impede formation of stable 14-3-3·cdc25C complexes, in the absence of a negatively charged phosphate group on Ser^{216}.

MP51 also interacts with cyclins A and B with an affinity similar to that for 14-3-3ζ. We have shown that this interaction is primarily mediated through the P-box motif of cyclins, providing the first direct biochemical evidence of an interaction between cdc25 phosphatases and the P-box of cyclins. This interaction was not affected by phosphorylation of Ser^{22}, suggesting that the residues in MP51 involved in this interaction are different from those that interact with 14-3-3ζ. However, phosphorylation of MP51, N-ter, and full-length cdc25C clearly favors their interaction with 14-3-3 over that with cyclins both *in vitro* and *in vivo*. This suggests that phosphorylation induces conformational changes in the MP51 domain of cdc25C that favor 14-3-3 binding, which in turn renders the residues involved in interactions with cyclin B1 inaccessible. From these data, we conclude that MP51 is a bi-functional domain of human cdc25C capable on the one hand of interacting with 14-3-3 proteins, through which control of subcellular localization is exerted, and of interacting with cyclins, on the other hand, thereby targeting cdc25C to cyclin-dependent kinases and promoting its mitotic function.

Structural Characterization of MP51—Cdc25 phosphatases are composed of a highly conserved C-terminal catalytic domain and an N-terminal regulatory domain, specific to each cdc25 isoform. Although the structures of the C-terminal domain of human cdc25A and cdc25B have been solved (50, 51), no structural information is available yet for the N-terminal domain of these phosphatases. Based on NMR data and on structural predictions, we have elaborated a structural model of MP51, which constitutes the first structural data of a subdomain of the N terminus of human cdc25C. MP51 can be described as an elbow-shaped entity formed by two independent α-helical domains, separated by a non-structured intervening loop that carries the two critical phosphorylation sites Ser^{20} and Ser^{22} (corresponding to Ser^{214} and Ser^{216} in human cdc25C) as well as the consensus 14-3-3 binding site. This structure is induced upon binding of 14-3-3ζ and can be mimicked by a hydrophobic environment using organic solvents. Our data reveal that residues of the bipartite NLS of human cdc25C are located in part in the amphipathic α2-helix and in part in the unfolded C terminus of the peptide and are all located on the same side of the structure of MP51. *In vivo*, this NLS is therefore presumably accessible for binding to the α-importin receptor. In contrast, using the structure of 14-3-3-peptide complexes (25, 48, 49) as a template for docking MP51 to 14-3-3, the α2-helix of MP51 appears to be buried inside the cleft of the 14-3-3 dimer, thus rendering the NLS completely inaccessible for recognition by the nuclear import machinery, consistent with the recent observation by Kumagai and Dunphy (28) that 14-3-3 binding reduces the ability of *Xenopus* cdc25 to associate with α-importin.

Phosphorylation of MP51 on Ser^{22} did not induce any dramatic modifications in its overall structure. However, this phosphorylation significantly increased the affinity of MP51 for 14-3-3 ζ and enabled 14-3-3 ζ to displace MP51P from preformed MP51P-cyclin B1 complexes, suggesting that some conformational changes must occur. In Raf-1-derived phosphopeptides complexed with 14-3-3, Pro at the position +2 in the R*S*X*S*X**P** motif (in bold) adopts a cis conformation, which reinforces the interaction with 14-3-3 (25, 48). NMR analysis of MP51 and MP51P reveals that in both peptides all the residues are in trans, indicating that phosphorylation of Ser^{22} is not

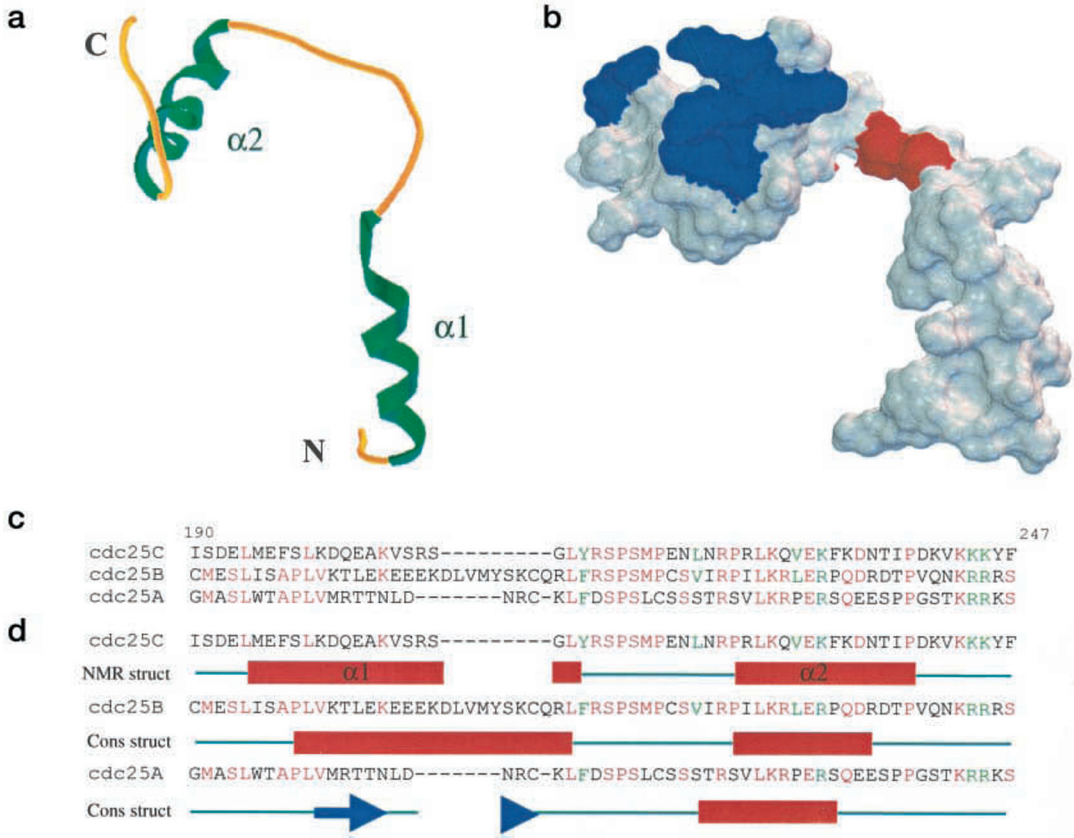

FIG. 6. **Structural model of MP51.** *a*, ribbon representation of MP51. The three-dimensional model of MP51 was elaborated based on NMR coordinates using Discover and Insight II. MP51 folds into two α-helices, α1 and α2. *b*, molecular surface representation of MP51. The residues involved in the putative NLS are shown in *blue*, and phosphorylation sites Ser^{20} and Ser^{22} are in *red*. *c*, sequence alignments of the 14-3-3 binding region of the three human cdc25 isoforms. *Red residues* are conserved in at least two cdc25 isoforms, and *green residues* present conserved physico-chemical characteristics. *d*, comparison of the secondary structure of the three human cdc25 isoforms. The secondary structure of cdc25A and cdc25B were predicted as described under "Experimental Procedures." The secondary structure of cdc25C corresponds to that obtained by NMR. α-Helices are represented as *red boxes*, and β-sheets are represented by *blue arrows*. *Red* and *green* residues are as in *panel c*.

responsible for an induced, stabilizing isomerization of Pro^{24}. Hence, we propose that if such an isomerization takes place in this mode 1 phosphopeptide, it must be induced by 14-3-3 binding.

Extension of the Model to Full-length cdc25C—The structural and functional models proposed above can be extended to full-length human cdc25C so as to reconcile the structural and binding properties of MP51 with the phosphorylation-dependent regulation of the subcellular localization and mitotic activity of full-length human cdc25C. Residues 195 to 244 of human cdc25C are likely to adopt the same bipartite helical fold as MP51, as they are located in a highly hydrophobic environment provided by the rest of cdc25C protein. As such, phosphorylation sites Ser^{214} and Ser^{216} as well as the 14-3-3ζ binding site would lie on an accessible, non-structured loop. *In vivo*, phosphorylation of Ser^{216} is required for binding of 14-3-3ζ to cdc25C, presumably by disrupting sterical hindrances in the full-length protein but additionally by inducing a stabilizing isomerization of Pro^{218}. High affinity binding of 14-3-3 to cdc25C would prevent mitotic activation of this phosphatase in a dual fashion, on the one hand by preventing the nuclear localization of cdc25C by burying its NLS within the channel of the 14-3-3 dimer, and on the other hand by precluding interactions with other proteins, in particular cyclins. We propose that *in vivo*, during interphase, a large fraction of cdc25C is phosphorylated on Ser^{216} by C-TAK1 and rapidly complexed to 14-3-3, which masks the NLS as well as residues required for interaction with cyclin B, and thus prevents its nuclear localization and cyclin binding. As Ser^{216} is deeply buried within the 14-3-3 dimer, we suggest that dissociation of 14-3-3 and not phospho-Ser^{216} dephosphorylation, is the first step in the mechanism of cdc25C activation at mitosis. This would on the one hand render the NLS accessible for recognition by the nuclear import machinery and, on the other, enable interactions with cdc2-cyclin B complexes. Dephosphorylation of Ser^{216} is probably required before cyclin B1 binds cdc25C, so as to prevent competitive, re-binding of 14-3-3. What promotes disruption of the highly stable 14-3-3·cdc25C complex still remains to be determined. Our data clearly exclude the possibility of cyclins displacing 14-3-3 from cdc25C. As the *in vivo* activation of cdc25C at the G_2/M transition is dependent on phosphorylation at mitotic sites, we suggest that disruption of the 14-3-3·cdc25C complex may be regulated by this phosphorylation.

Acknowledgments—We thank Dr. C. H. McGowan for providing human-GST-cds1. We thank both Dr. C. H. McGowan and Dr. S. I. Reed for critical reading of the manuscript, helpful suggestions, and comments. We thank Dr. L. Chaloin for technical advice. We thank Dr. M. Dorée for continuous support.

REFERENCES

1. Dorée, M., and Galas, S. (1994) *FASEB J.* **8,** 1114–1121
2. Morgan, D. O. (1997) *Annu. Rev. Cell Dev. Biol.* **13,** 261–291
3. Furnari, B., Rhind, N., and Russell, P. (1997) *Science* **277,** 1495–1497
4. Sanchez, Y., Wong, C., Thoma, R. S., Richman, R., Wu, Z., Piwnica-Worms, H., and Elledge, S. J. (1997) *Science* **277,** 1497–1501
5. Peng, C.-Y., Graves, P. R., Thoma, R. S., Wu, Z., Shaw, A. S., and Piwnica-Worms, H. (1997) *Science* **277,** 1501–1505
6. Nagata, A., Igarashi, M., Jinno, S., Suto, K., and Okayama, H. (1991) *New Biol.* **3,** 959–968
7. Galaktionov, K., Lee, A. K., Eckstein, J., Draetta, G., Meckler, J., Loda, M.,

and Beach, D. (1995) *Science* **269,** 1575–1577
8. Galaktionov, K., and Beach, D.(1991) *Cell* **67,** 1181–1194
9. Jinno, S., Suto, K., Nagata, A., Igarashi, M., Kanaoka, Y., Nojima, H., and Okayama, H.(1994) *EMBO J.* **13,** 1549–1556
10. Hoffmann, I., Draetta, G., and Karsenti, E. (1994) *EMBO J.* **13,** 4302–4310
11. Gabrielli, B. G., De Souza, C. P. C., Tonks, I. D., Clark, J. M., Hayward, N. K., and Ellem, K. A. O. (1996) *J. Cell Sci.* **109,** 1081–1093
12. Karlsson, C., Katich, S., Hagting, A., Hoffmann, I., and Pines, J. (1999) *J. Cell Biol.* **146,** 573–583
13. Sadhu, K., Reed, S. I., Richardson, H., and Russell, P. (1990) *Proc. Natl. Acad. Sci. U. S. A.* **87,** 5139–5143
14. Millar, J. B. A., Blevitt, J., Gerace, L., Sadhu, K., Featherstone, C., and Russell, P. (1991) *Proc. Natl. Acad. Sci. U. S. A.* **88,** 10500–10504
15. Hoffmann, I., Clarke, P. R., Marcote, M. J., Karsenti, E., and Draetta, G. (1993) *EMBO J.* **12,** 53–63
16. Strausfeld, U., Fernandez, A., Capony, J.-P., Girard, F., Lautredou, N., Derancourt, J., Labbe, J.-C., and Lamb, N. J. C. (1994) *J. Biol. Chem.* **269,** 5989–6000
17. Lamb, N. J. C., Morris, M. C., and Fernandez, A. (1994) *Adv. Protein Phosphatases* **8,** 133–151
18. Ogg, S., Gabrielli, B., and Piwnica-Worms, H.(1994) *J. Biol. Chem.* **269,** 30461–30469
19. Peng, C. Y., Graves, P. R., Ogg, S., Thoma, R. S., Byrnes, M. J., Wu, Z., Stephenson, M. T., and Piwnica-Worms, H. (1998) *Cell Growth Differ.* **9,** 197–208
20. Blasina, A., Van de Weyer, I., Laus, M. C., Luyten, W. H. M. L., Parker, A. E., and McGowan, C. H. (1999) *Curr. Biol.* **9,** 1–10
21. Mastuoka, S., Huang, M., and Elledge, S. (1998) *Science* **282,** 1893–1897
22. Kumagai, A. Guo, Z., Emami, K. H., Wang, S. X., and Dunphy, W. G. (1998) *J. Cell Biol.* **142,** 1559–1569
23. Zeng, Y., Forbes, K. C., Wu, Z., Moreno, S., Piwnica-Worms, H., and Enoch, T. (1998) *Nature* **395,** 507–510
24. Muslin, A. J., Tanner, J. W., Allen, P. M., and Shaw A. S. (1996) *Cell* **84,** 889–897
25. Yaffe, M. B., Rittinger, K., Volinia, S., Caron, P. R., Aitken, A., Leffers, H., Gamblin, S. J., Smerdon, S. J., and Cantley, L. C. (1997) *Cell* **91,** 961–971
26. Lopez-Girona, A., Furnari, B., Mondesert, O., and Russell, P. (1999) *Nature* **397,** 172–175
27. Kumagai, A., Yakowec, P. S., and Dunphy, W. G. (1998) *Mol. Biol. Cell* **9,** 345–354
28. Kumagai, A., and Dunphy, W. G. (1999) *Genes Dev.* **13,** 1067–1072
29. Yang, J., Winkler, K., Yoshida, M., and Kornbluth, S. (1999) *EMBO J.* **18,** 2174–2183
30. Dalal, S. N., Schweitzer, C. M., Gan, J., and DeCaprio, J. A. (1999) *Mol. Cell. Biol.* **19,** 4465–4479
31. Morris, M. C., Méry, J., Heitz, A., Heitz, F., and Divita, G. (1999) *J. Pept. Sci.* **5,** 263–271
32. Chaloin, L., Vidal, P., Heitz, A., Van Mau, N., Méry, J., Divita, G., and Heitz, F. (1997) *Biochemistry* **36,** 11179–11187
33. Griesinger, C., Otting, G., Wüthrich, K., and Ernst, R. R. (1998) *J. Am. Chem. Soc.* **110,** 7870–7872
34. Kumar, A., Ernst, R. R., and Wüthrich, K. (1980) *Biochem. Biophys. Res. Commun.* **95,** 1–6
35. Kontaxis, G., Stonehouse, J., Laue, E. D., and Keeler, J. (1994) *J. Magn. Reson.* **111,** 70–76
36. Wüthrich, K.(1996) in *NMR of Proteins and Nucleic Acids*, John Wiley & Sons, Inc., New York
37. Thanabal, V., Omencinsky, D. O., Reily, M. D., and Cody, W. L (1994) *J. Biomol. NMR* **4,** 47–59
38. Guermeur, Y., Geourjon, C., Gallinari, P., and Deleage, G. (1999) *Bioinformatics* **15,** 413–421
39. Heitz, F., Morris, M. C., Fesquet, D., Cavadore, J.-C., Dorée, M., and Divita, G. (1997) *Biochemistry* **36,** 4995–5003
40. Morris, M. C., and Divita, G. (1999) *J. Mol. Biol.* **286,** 475–487
41. Xiao, B., Smerdon, S. J., Jones, D. H., Dodson, G. G., Soneji, Y., Aitken, A., and Gamblin, S. J. (1995) *Nature* **376,** 188–191
42. Liu, D., Bienkowska, J., Petosa, C., Collier, R. J., Fu, H., and Liddington, R. (1995) *Nature* **376,** 191–194
43. Zheng, X.-F., and Ruderman, J. V. (1993) *Cell* **75,** 155–164
44. Brown, N. R., Noble, M. E., Lawrie, A. M., Morris, M. C., Tunnah, P., Divita, G., Johnson, L. N., and Endicott, J. A. (1999) *J. Biol. Chem.* **274,** 8746–8756
45. Wright, P. E., and Dyson, H. J. (1999) *J. Mol. Biol.* **293,** 321–331
46. Wishart, D. S., and Sykes, B. D.(1994) *Methods Enzymol.* **239,** 363–392
47. Dyson, J. H., and Wright, P. E. (1991) *Annu. Rev. Biophys. Biophys. Chem.* **20,** 519–538
48. Rittinger, K., Budman, J., Xu, J., Volinia, S., Cantley, L. C., Smerdon, S. J., Gamblin, S. J., and Yaffe, M. B. (1999) *Mol. Cell* **4,** 153–166
49. Petosa, C., Masters, S. C., Bankston, L. A., Pohl, J., Wang, B., Fu, H., and Liddington, R. C. (1998) *J. Biol. Chem.* **273,** 16305–16310
50. Fauman, E. B. Cogswell, J. P., Lovejoy, B., Rocque, W. J., Holmes, W., Montana, V. G., Piwnica-Worms, H., Rink, M. J., and Saper, M. A. (1998) *Cell* **93,** 617–625
51. Reynolds, R. A., Yem, A. W., Wolfe, C. L., Deibel, M. R. Jr., Chidester, C. G., and Watenpaugh, K. D. (1999) *J. Mol. Biol.* **293,** 559–568